EUV Plasma Source with IR Power Recycling

Kenneth C. Johnson kjinnovation@earthlink.net 1/6/2016 (first revision)

Abstract

Laser power requirements for an EUV laser-produced plasma source can be reduced by using power-recycling optics to reflect plasma-scattered IR radiation back onto the plasma. Previously proposed spherical retroreflective mirrors can be used to form an inverted image of the plasma on itself, but an erect (non-inverted) image would be more tolerant of positional alignment errors. Erect-imaging optical design alternatives for power recycling are described in this paper.

Introduction

A laser-produced plasma (LPP) produces extreme ultraviolet (EUV) radiation from high-energy ionization of a laser-vaporized target such as a tin droplet. Typically, a stream of tin droplets is irradiated by a pulsed CO_2 laser at a 10.6-μm infrared (IR) wavelength, producing EUV radiation at wavelength 13.5 nm. The EUV output is focused by an elliptical collector mirror onto an intermediate focus (IF).

Ref's. 1 and 2 describe power-recycling collector optics, which reduce laser power requirements of an LPP source by retroreflecting plasma-scattered IR and other out-of-band radiation back onto the plasma. A limitation of these systems is that they form an inverted image of the plasma on itself, which makes the system sensitive to positional misalignment between the plasma and retroreflector (e.g., a positional displacement of the plasma causes its self-image to move in the opposite direction, away from the plasma). Ideally, the system would produce an erect (non-inverted) plasma image, which would tend to follow any positional variations of the plasma relative to the imaging optics. The retroreflectors' positional alignment tolerances would be significantly relaxed. Also, EUV power stability would be improved because variations in the plasma position would not affect power recycling efficiency. This paper describes two types of erect-image retroreflector systems: a cat's-eye lens/mirror array and a corner-cube mirror array.

Cat's-Eye Array

Figure 1 illustrates a variation of Figure 5 in Ref. 2 in which the spherical retro mirrors are double-shell reflectors, each comprising a transmitting inner shell and a reflecting outer shell. The enlarged detail view in Figure 1 shows a cross-sectional view of a double-shell reflector. An array of converging lenses on the inner shell images the plasma onto foci on the outer shell, and an array of concave mirrors on the outer shell retroreflects the plasma images back through the lenses. Each lens is paired with a corresponding mirror, and the two in combination operate as a cat's-eye retroreflector. Accurate retroreflection is maintained even as the plasma position varies (as indicated by the dashed ray lines and direction arrow in Figure 1).

The beam reflected from each cat's-eye element has a diffraction-limited angular spread of approximately λ / w, where λ is the wavelength and w is the lens aperture width. The

diffractive spread should be smaller than the plasma subtend angle δ at the reflector: $\lambda / w < \delta$. w would typically be significantly larger than 10 mm. At the 10.6-μm IR wavelength, this results in a diffractive spread less than 1 mrad ($\lambda / w < 0.001$), which is comparable to δ for typical LPP geometries.

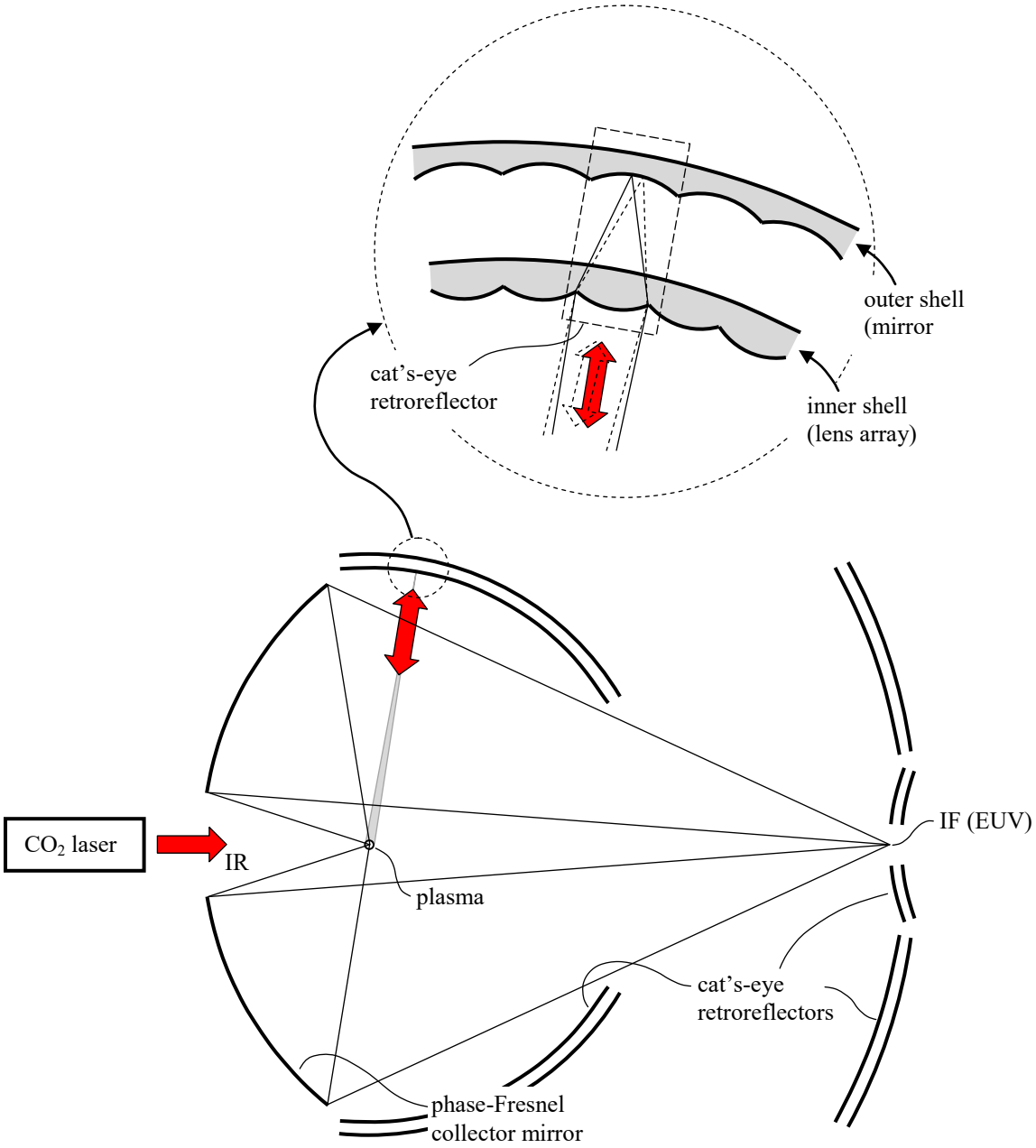

Figure 1. IR power recycling with cat's-eye retroreflectors.

If the retroreflector array is accurately constructed and aligned to preserve phase coherence between cat's-eye elements at the plasma center point, then the array operates as a diffraction grating, which concentrates most or all of the reflected radiation into a single

diffraction order. The aperture diffraction spread of a single order can be much smaller than a single element's aperture diffraction limit. But the alignment tolerance required to maintain phase coherence would be comparable to that of the spherical-shell reflector described in Ref. 2, so the cat's-eye system would have no advantage over the Ref. 2 design.

A periodic array of cat's-eye reflectors generally operates as a diffraction grating that concentrates most of the reflected energy into multiple diffraction orders close to the geometric-optics reflected ray direction. The angular separation between diffraction orders is approximately λ / w, which should be small in relation to δ to ensure that the reflected energy is concentrated onto the plasma. Thus, the condition $\lambda / w < \delta$ holds irrespective of whether coherent interactions between cat's-eye elements are considered.

The Figure-1 configuration can be simplified in several ways. The space between the two shells could be filled with solid dielectric material, in which case the outer shell would simply be a reflective mirror coating formed on the inner shell's back side. The lenses and mirrors can be replaced by phase-Fresnel elements (e.g. using a lithographic patterning process). The spherical-shell substrates can be replaced by flat plates, using off-axis lenses or mirrors to accommodate off-axis illumination on the plates' peripheral region. For example, Figure 2 shows a cross-sectional view of a flat-plate design using phase-Fresnel lenses and off-axis, phase-Fresnel mirrors.

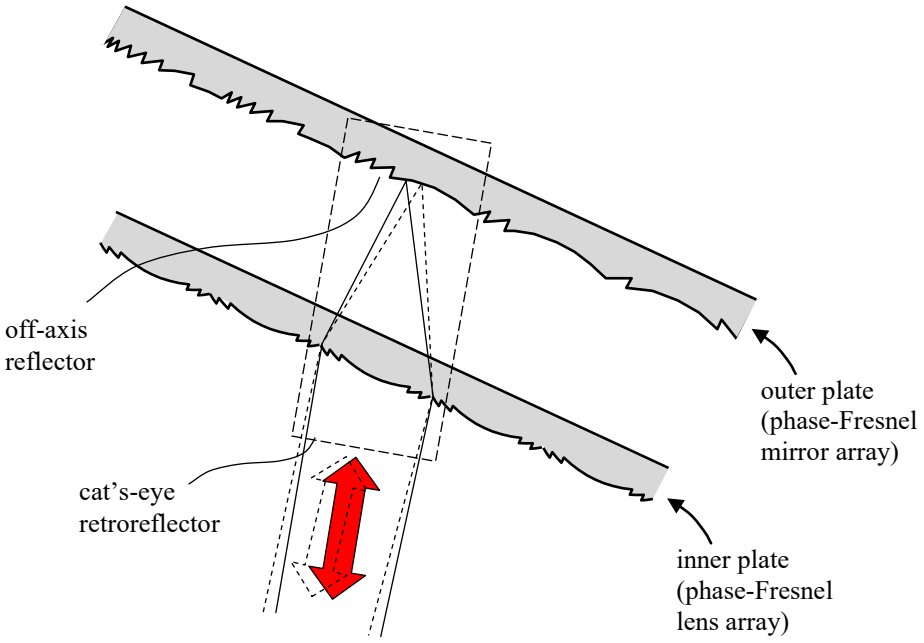

Figure 2. Flat-plate cat's-eye retroreflector design with phase-Fresnel optics.

The retroreflector mirror elements need not necessarily be curved. Figure 3 illustrates a flat-plate design using off-axis lenses and a flat mirror surface. Each lens focuses the plasma's center point into a convergent light cone with the cone axis normal to the mirror. There may be some slight vignetting of the reflected light cone by the lens aperture when the plasma position changes, but accurate plasma self-imaging will still be maintained.

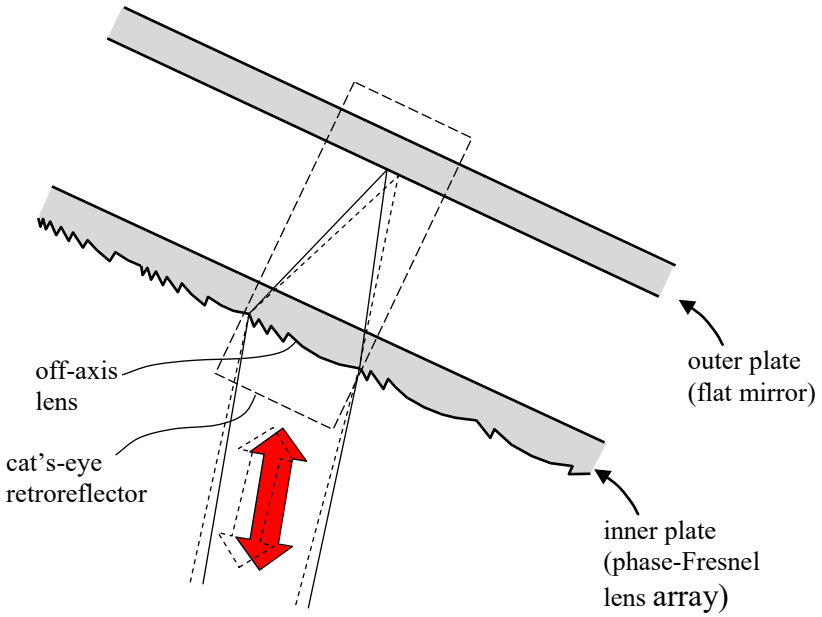

Figure 3. Cat's-eye retroreflector array with flat mirror.

The cat's-eye array elements need not be contiguous; they could be discrete components as illustrated in Figure 4. In this illustration, each cat's-eye element is a solid glass element with an on-axis, convex lens surface and a flat, reflective back surface. The lens axes are aligned to the plasma center, but the alignment tolerance is much looser than the plasma subtend angle.

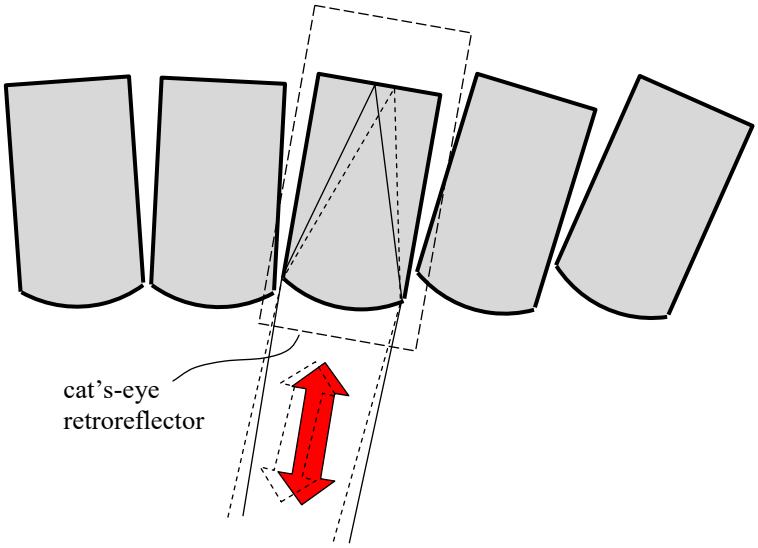

Figure 4. Discontiguous cat's-eye array.

A cat's-eye array can efficiently retroreflect the 10.6-μm IR radiation to the plasma, but may not be able to retroreflect much of the other out-of-band radiation due to chromatic dispersion in the lens. The system could use a hybrid diffractive/refractive lens design (similar to a phase-Fresnel lens, but on a curved substrate), although this would only allow accurate point imaging at two wavelengths. Also, infrared lens materials (e.g. zinc selenide, ZnSe, for 10.6-μm IR) have transmittance limits at shorter wavelengths. The corner-cube designs described below overcome these limitations.

Corner-Cube Reflector Array

Figure 5 shows another variation of Figure 5 in Ref. 2 in which the spherical retro mirrors comprise corner-cube retroreflector arrays. The mirrors are illustrated schematically by a sawtooth profile, but each retroreflector is a three-surface, corner-cube element.

Figure 6 illustrates a portion of a conventional corner-cube array, one element of which is shaded. From this perspective the incident beam reflects off the top of the array. Each corner cube's three reflective surfaces are planar, square, and mutually orthogonal; and the cube's aperture projection in the incidence direction is hexagonal. The device operates to retroreflect a collimated beam directed approximately parallel to an optical axis, which is oriented at the same angle (approximately 54.7°) to all three reflector surface normals.

A conventional corner-cube design can be modified to achieve accurate self-imaging of an axial point at finite conjugate by making the reflector surfaces slightly concave, as described in Ref. 3 (e.g. see Figure 4 in Ref. 3). The surface geometry has sufficient degrees of freedom to achieve perfect geometric self-imaging of the plasma center point (although the optimal surface shape might not be exactly spherical as described in Ref. 3). Off-axis aberrations would be insignificant in comparison to the plasma size, provided that the reflector elements are sufficiently small. (As with the cat's-eye array, the corner-cube aperture size may need to be significantly larger than 10 mm to avoid excessive image degradation from aperture diffraction. But with typical LPP dimensional scales, the corner cubes would nevertheless be small enough to limit off-axis geometric aberrations.)

The enlarged detail view in Figure 5 shows a cross-section of a corner-cube array formed in a solid glass shell with the reflectors formed on its back side. This type of device requires no reflective mirror coating; it can operate via total internal reflection. However, it could only retroreflect out-of-band radiation within a limited wavelength band because of the spectral transmittance limitations of common optical materials such as ZnSe. Alternatively, front-surface reflectors could be formed as recessed, pyramidal cavities with metal or dielectric-coated reflector surfaces. This avoids bulk transmittance losses, although the spectral reflectance of common reflective coatings could be a limitation.

Figure 7 illustrates an alternative to the Figure-5 configuration, which uses conventional, flat-face corner cubes. Collimating lenses (e.g. phase-Fresnel elements) on the reflector shell's inner surface collimate rays from the plasma center point, and these rays are retroreflected by the corner-cubes. If front-surface reflectors are used, then the collimating lenses can be formed on a separate, inner shell. (An advantage of this design over the Figure-1 double-shell configuration

is that the shells need not be widely separated to accommodate the lens focal lengths. Chromatic dispersion would probably be insignificant because the collimating lenses have very low optical power.)

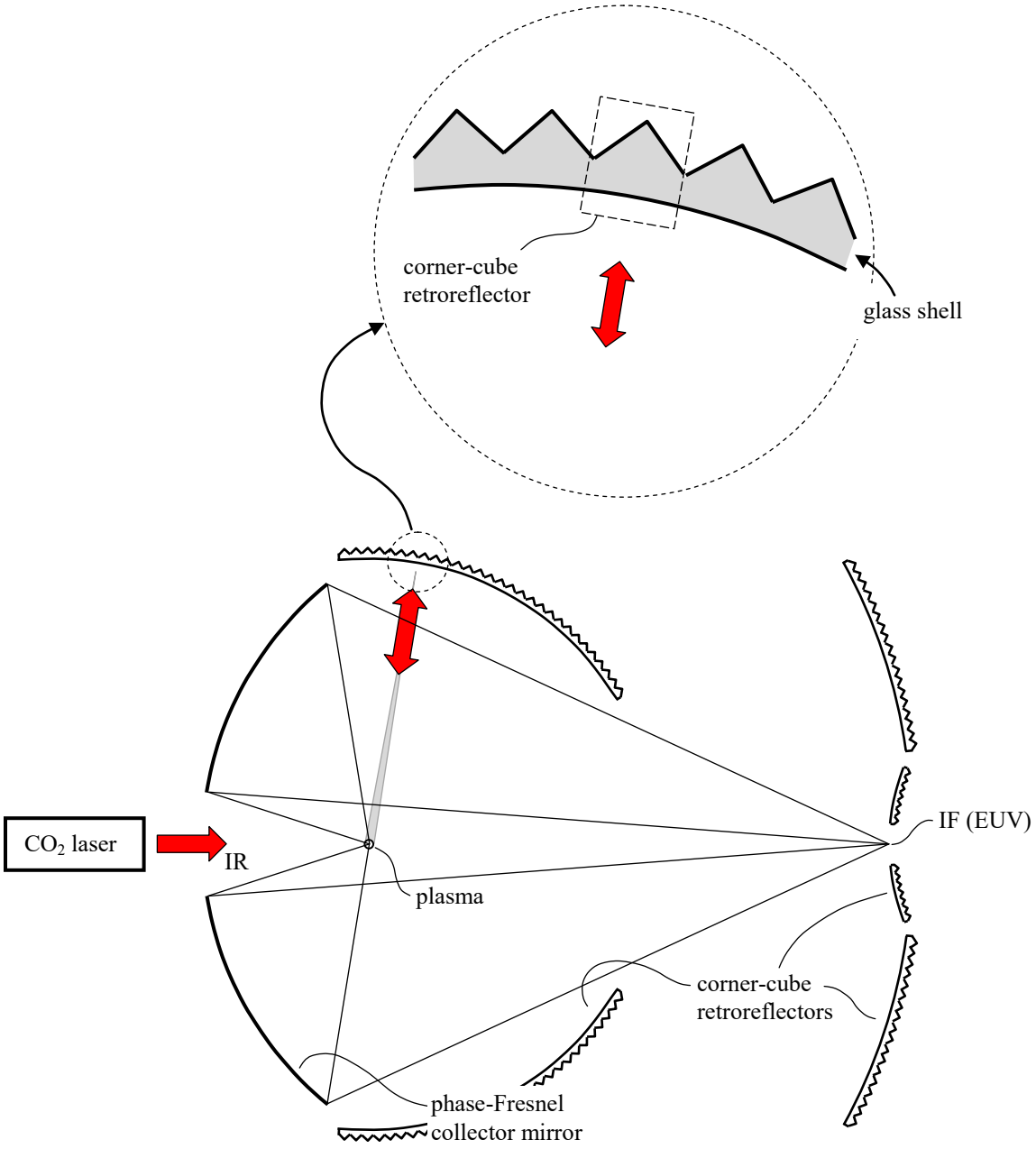

Figure 5. IR power recycling with corner-cube retroreflectors.

The corner-cube arrays can be formed in a flat-plate configuration analogous to the flat-plate cat's-eye design of Figure 2. In this case the corner-cube optical axes would be tilted relative to the plate normal over the peripheral portions of the plate to accommodate the incident beam divergence, as illustrated in Figure 8. Alternatively, off-axis collimating lenses can be

used to collimate the beams in a common direction, allowing the use of a uniformly periodic array of flat-face corner cube reflectors; see Figure 9.

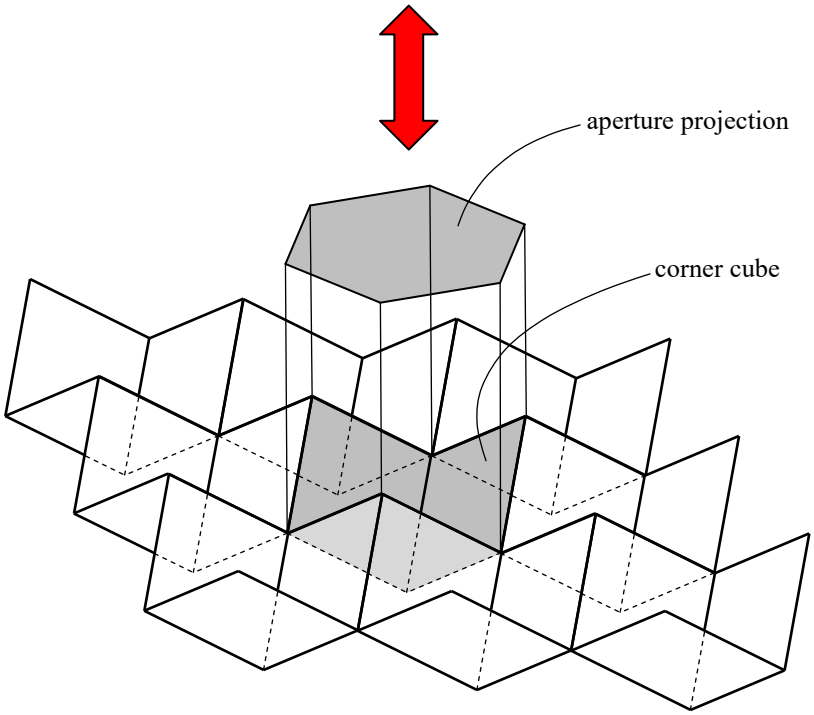

Figure 6. Corner-cube retroreflector array.

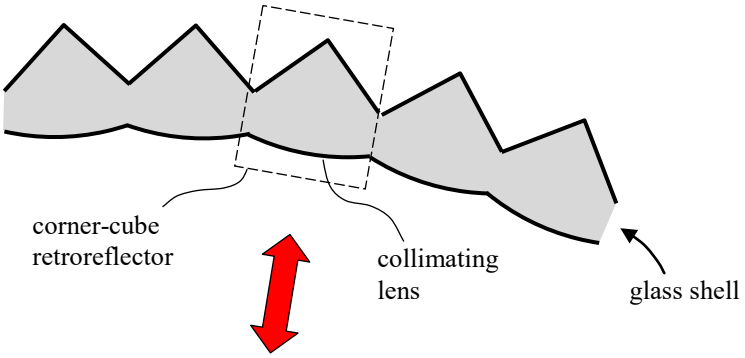

Figure 7. Flat-face corner-cube retroreflectors with collimating lenses.

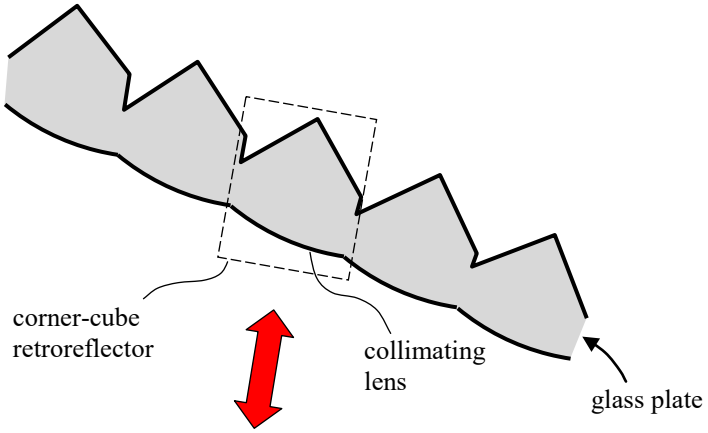

Figure 8. Flat-plate corner-cube array with tilted corner-cubes.

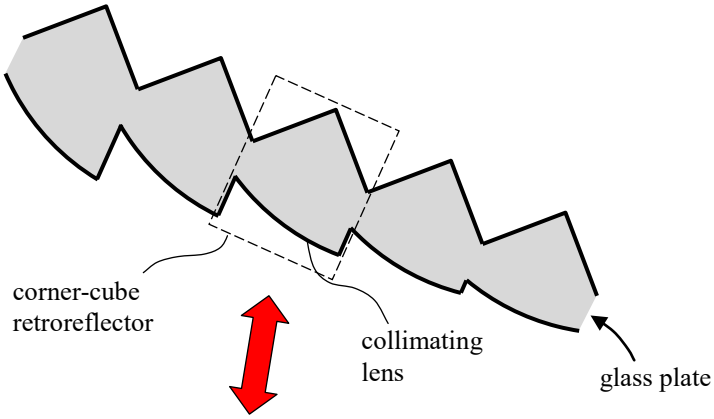

Figure 9. Flat-plate corner-cube array with off-axis collimating lenses.

A corner-cube reflector array can be fabricated by tiling an array of hexagonal-section bar segments, each of which has three precision-machined and polished corner-cube reflector surfaces on its end. The bar segments can be fused or bonded to a common substrate, or can be used as a replication master for manufacturing the reflector array (e.g. by molding or electroplating).

The array can also be formed as a collection of discrete, non-contiguous corner-cube elements, as illustrated schematically in Figure 10. In this configuration the corner-cube elements are front-surface reflectors with slightly curved surfaces similar to the design described in Ref. 3.

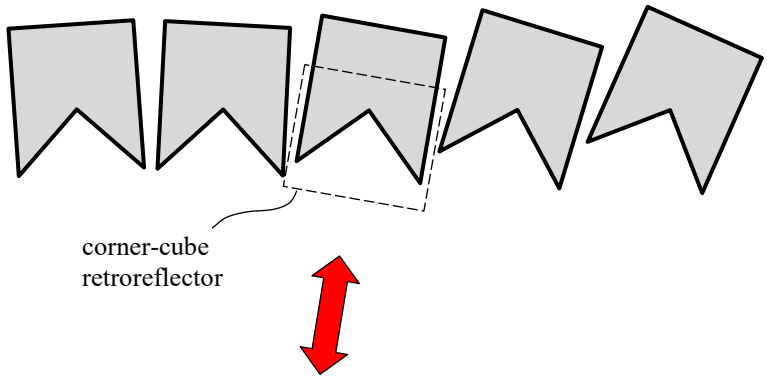

Figure 10. Discontiguous corner-cube array.

Integration with Spectral Purity Filter

Either a cat's-eye or corner-cube reflector design can be used for the retro mirror in the spectral filter system illustrated in Figure 6 of Ref. 2. (In this case the incident rays on the retro mirror are convergent to point P in the figure, so the collimating lenses in the corner-cube configuration of Figure 7 herein would be concave, negative-power elements on a convex glass shell.)

The grating line density on the periphery of the phase-Fresnel collector mirror can be reduced by designing some spherical aberration into the focused IR beam, as illustrated in Figure 11. IR rays reflected from the collector mirror near the center (at radius $R_{\min}$) intercept the optical axis at point P, as in Figure 6 of Ref. 2. But rays reflecting from the periphery (at radius $R_{\max}$) cross the axis at point P', closer to the IF. (Other rays cross the axis at intermediate points.) This reduces the angle between the reflected IR and diffracted EUV rays, resulting in a lower grating line density. The tradeoff to this advantage is that the retroreflector will need to operate over a greater angular range, possibly resulting in compromised power recycling performance.

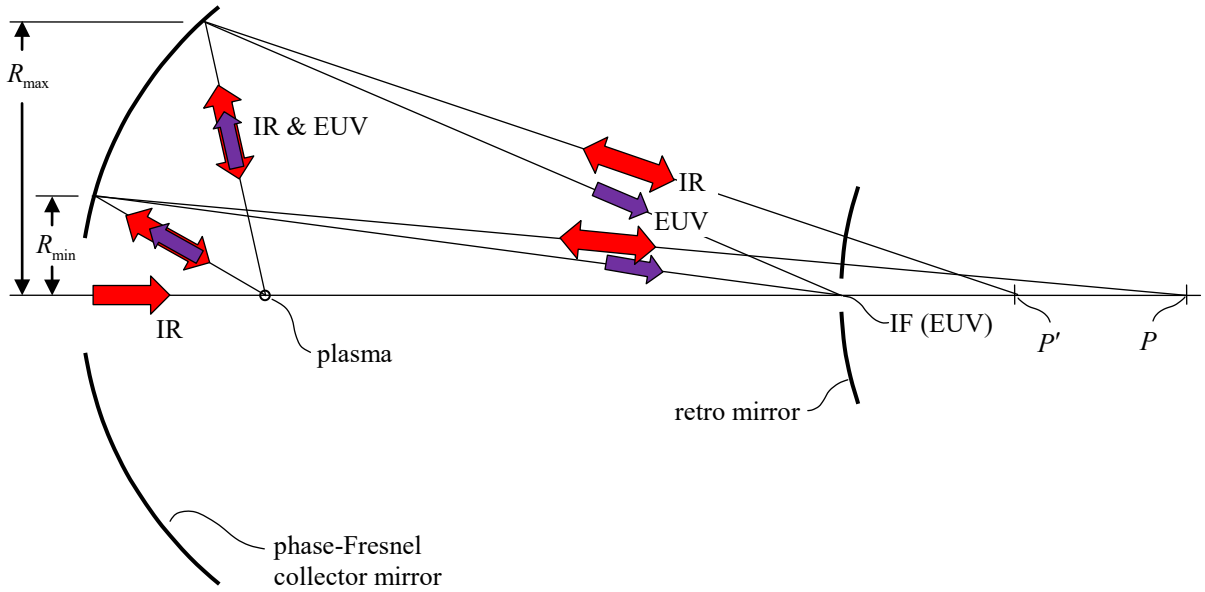

Figure 11. Spectral filter with spherically aberrated IR focus.

References

1. Bayraktar, Muharrem, Fred A. van Goor, Klaus J. Boller, and Fred Bijkerk. “Spectral purification and infrared light recycling in extreme ultraviolet lithography sources.” *Optics express* 22, no. 7 (2014): 8633-8639.

2. Kenneth C. Johnson. “EUV Spectral Purity Filter for Full IR-to-VUV Out-of-Band Rejection, with IR Power Recycling.” 2015. http://vixra.org/abs/1512.0295

3. Macken, John. “Corner cube utilizing generally spherical surfaces.” U.S. Patent 4,941,731, issued July 17, 1990.